Macromolecular Chemistry and Physics
www.mcp-journal.de

Incorporation of Magnetic Nanoparticles in Poly(Methyl Methacrylate) Nanocapsules

*Ludmila I. Ronco, Paulo E. Feuser, Alexandre da Cas Viegas, Roque J. Minari, Luis M. Gugliotta, Claudia Sayer, and Pedro H. H. Araújo**

Magnetic nanoparticles (MNPs) encapsulated in polymeric systems are promising materials for hyperthermia treatments and targeting drug delivery in cancer therapy. To improve the encapsulation efficiency of therapeutic drugs, high amounts of fatty acids can be incorporated into the polymer matrix. The effect of the monounsaturated fatty acid oleic acid (OA)/Crodamol (triacylglycerol of saturated fatty acids) ratio in the incorporation of MNPs in poly(methyl methacrylate) (PMMA) nanocapsules by miniemulsion polymerization is investigated. The OA/Crodamol ratio affects polymerization kinetics, polymer microstructure, and nanocapsules morphology. Furthermore, MNPs are efficiently encapsulated in PMMA nanocapsules with high Crodamol content while preserving their super-paramagnetic behavior with considerable magnetization saturation values.

1. Introduction

Iron oxide magnetic nanoparticles (MNPs), which consist mainly of magnetite (Fe_3O_4), present great potential in biomedical applications, such as, targeted drug delivery, hyperthermia, and magnetic resonance imaging.[1–5] For these applications, MNPs must combine properties of high magnetic saturation, super-paramagnetic properties and biocompatibility. The encapsulation of MNPs in polymeric particles aims to protect and to prevent aggregation of MNPs[6] and at the same time can ensure the mobility of the polymeric particles when a magnetic field is applied, enabling their use for targeted delivery of therapeutic agents[7–9] in combination with hyperthermia in cancer treatments.[10–12]

Dr. L. I. Ronco, Prof. R. J. Minari, Prof. L. M. Gugliotta
Instituto de Desarrollo Tecnológico para la Industria Química (INTEC UNL-CONICET)
Güemes 3450, Santa Fe 3000, Argentina
Dr. P. E. Feuser, Prof. C. Sayer, Prof. P. H. H. Araújo
Department of Chemical Engineering and Food Engineering
Federal University of Santa Catarina
Florianopolis, SC 88040-900, Brazil
E-mail: pedro.h.araujo@ufsc.br
Prof. A. da Cas Viegas
Department of Physic
Federal University of Santa Catarina
Florianopolis, SC 88040-900, Brazil
The ORCID identification number(s) for the author(s) of this article can be found under https://doi.org/10.1002/macp.201700424.

DOI: 10.1002/macp.201700424

Different types of nanoparticle morphologies could be employed to combine hyperthermia treatment and drug delivery such as: (i) magnetic core/polymer shell nanoparticles with encapsulated drug within the polymeric shell; and (ii) nanocapsules with a liquid core surrounded by a polymer shell, containing drug and MNPs distributed in one or both phases. These types of nanoparticle morphologies could also satisfy different requirements in spatio-temporal control delivery of therapeutic agents.[4] Regarding this, Liu and Kitamoto[13] reported the synthesis of nanoparticles with a magnetic FeOx/silica core and a thermo-responsive polymer (hydroxypropyl cellulose) shell, with potential application as thermally controlled drug release carrier.

In recent years, miniemulsion polymerization has received great attention for the synthesis of nanocapsules, which appear as promising candidates for the controlled and targeted delivery of active compounds in a variety of biomedical applications.[14] During miniemulsion polymerization, nanocapsules are formed by initially dispersing droplets of monomer and costabilizer in water using a suitable surfactant, and with the help of high shear. The costabilizer presents the lowest water solubility of all components in the system and introduces a counterforce energy of mixing that counteracts the interfacial energy responsible for molecular diffusion degradation (Ostwald ripening). The particle shell is formed during the polymerization stage, when the growing polymer chains become immiscible in the dispersed phase and phase-separate from the costabilizer-rich phase. Due to the polymer lower interfacial energy with water when compared to the costabilizer, it will tend to partition preferentially to the water interface, forming particles with a polymer shell and a core composed of the costabilizer. In order to obtain nanocapsules for biomedical applications, different biocompatible oils could be employed as costabilizers, such as caprylic/capric triglyceride[15,16] castor oil,[17] jojoba and andiroba oils,[18] linoleic acid, and oleic acid.[19,20]

Miniemulsion polymerization has been used to encapsulate MNPs into polymeric nanoparticles in different polymeric matrixes such as polystyrene,[21] poly(styrene–butadiene),[22] poly(urea–urethane),[23] and poly(methyl methacrylate) (PMMA).[10,11,24–26] However, as far as the authors are aware, the incorporation of MNPs in polymer nanocapsules was not previously studied.

Usually, the first step for the encapsulation of MNPs by miniemulsion polymerization is the hydrophobization of their

surface using oleic acid. The MNPs coated with oleic acid are dispersed in the monomer droplets that act as a separate polymerization locus and thus lead to a similar concentration of MNPs in each droplet. After polymerization, a colloidal dispersion is obtained, still featuring uniform distribution of the MNPs in all polymeric nanoparticles[26] rendering direct miniemulsion polymerization an efficient encapsulation method of water insoluble materials.

The goals of this work were to synthesize and characterize MNPs incorporated in PMMA nanocapsules (MNPs–PMMA) for potential applications in targeted drug delivery and hyperthermia. Several reactions were carried out employing different contents of OA (monounsaturated fatty acid) and Crodamol (triacylglycerol of saturated fatty acids) as costabilizer (and to form the hydrophobic core). The effect of costabilizer type and of incorporation of MNPs on polymerization kinetics, nanocapsule morphology, polymer microstructure, and magnetic properties of synthesized nanocapsules was investigated.

2. Experimental Section

2.1. Materials

The following reactants were used to synthesize the MNPs: iron (III) chloride ($FeCl_3 \cdot 6H_2O$, 97–102% purity), iron (II) sulfate ($FeSO_4 \cdot 7H_2O$, >99% purity), and ammonium hydroxide (28–30% NH_3 basis) from Vetec Chemistry, and pure oleic acid (OA) from Lafan Quimica Fina Ltda. For the nanocapsule synthesis, methyl methacrylate (MMA, Vetec Chemistry, 99.5% purity) was used as monomer, Crodamol GTCC (caprylic/capric triglyceride, Croda) and OA as costabilizers, refined lecithin (Alfa Aesar) as surfactant, and azobisisobutyronitrile (AIBN, VETEC Chemistry) was the polymerization initiator. Hydroquinone (Nuclear) was used to stop the reaction after sample collection. The initiator AIBN was purified by recrystallization. All other reagents were employed directly as received, without further purification. In addition, distilled water was used throughout the work.

2.2. Synthesis of Oleic Acid Coated MNPs (MNPs–OA)

MNPs were synthesized by coprecipitation in aqueous phase as described by Feuser et al.[10] Briefly, $FeCl_3 \cdot 6H_2O$ and $FeSO_4 \cdot 7H_2O$ (mole ratio of 1:1.2) were dissolved in a beaker containing distilled water and under mechanical stirring at 800 rpm. Immediately after, a NH_4OH solution (11 mL) was added to the mixture. In order to disperse the synthesized MNPs in the nonpolar organic phase for the preparation of the miniemulsion and to achieve compatibility between them and the hydrophobic polymer, their surface was hydrophobized with OA. To this effect, 1 h after the addition of NH_4OH solution, OA (30 mL) was incorporated and stirring was continued for 30 min more. The MNPs coated with OA (MNPs–OA) were washed with ethanol and centrifuged three times to remove the excess of OA.

2.3. Nanocapsules Synthesis by Miniemulsion Polymerization

PMMA nanocapsules were synthesized by miniemulsion polymerization. In order to form the nanocapsules, the costabilizer, besides of retarding the diffusional degradation (Ostwald ripening), is also responsible for the formation of the particle liquid core. All miniemulsions were prepared with 20% of disperse (organic) phase. The organic phase for each experiment was composed of 60 wt% of MMA and different contents of Crodamol and OA. Also, 3% wbop (weight based on organic phase) of lecithin, 2% wbm (weight based on monomer) of AIBN; and 15% wbm of MNPs–OA (in the reactions in which MNPs were employed) were added to the organic phase. The aqueous phase was composed of distilled water. To produce the miniemulsion, the organic and aqueous phases were first mixed by magnetic stirring for 30 min, and the resulting preemulsion was sonified for 3 min using an ultrasound probe (Fisher Scientific, Sonic Dismembrator Model 500) at 70% of amplitude, in cycles of 10 s on and 5 s off. Then, batch polymerization reactions were carried out in 10 mL ampoules immersed in a thermostatic bath at constant temperature (70 °C) for 6 h.

2.4. Characterization

Samples were withdrawn along the reactions to measure: (i) monomer conversion (x) by gravimetry and (ii) average droplets (d_d) and particle (d_p) diameters and respective polydispersity index (PDI) by dynamic light scattering (DLS) using a Malvern Nanosizer. For DLS measurements, samples were diluted with distilled water saturated with MMA monomer, in order to avoid loss of monomer from droplets and particles to the continuous phase.

Thermogravimetric analysis (TGA) was performed to determine the wt% of magnetite in the nanocapsules. The MNPs–OA and PMMA nanocapsules were measured through TGA runs under nitrogen atmosphere at a heating rate of 10 °C min^{-1} between 20 and 800 °C.

The molecular weight distribution of PMMA and its averages (M_n and M_w) were determined by size exclusion chromatography. The measurements were carried out within a Waters 1515 chromatograph fitted with a differential refractometer (Waters 2414); and 2 poly(St/DVB) columns (HR 4E and HR 5E) from Waters Corp., of nominal fractionation range 10^3–10^7 g mol^{-1}). The chromatograph was calibrated with a set of 9 (Shodex) narrow polystyrene standards in the range 10^3–10^6 g mol^{-1}.

Fourier-transform infrared spectroscopy (FT-IR) was used to confirm the chemical structure of the MNPs–PMMA nanocapsules using a KBr pellet. The magnetic properties of MNPs–PMMA nanocapsules were measured at 300 K using a EV9 (MicroSense) electromagnet vibrating sample magnetometer (VSM).

PMMA nanocapsules morphologies were analyzed with a transmission electronic microscope (TEM), model JEM 2100F 100 kV. For TEM analysis, a drop of diluted sample (0.1 wt%) was placed on a 300 mesh carbon/Formvar-coated copper grid. After drying, samples were sputter-coated with a thin carbon film to avoid degradation of the PMMA under the electron beam.

Table 1. Conversion, molecular weight, and average droplet and nanocapsules size obtained in the absence and presence of magnetic nanoparticles.

Experiment[a)]	d_d [nm]	X [%]	M_n [kDa]	M_w [kDa]	d_p [nm]	PDI
$M_{60}O_{35}C_5$	169	73	28.3	69.4	173	0.10
$M_{60}O_{20}C_{20}$	166	88	35.1	93.7	177	0.10
$M_{60}O_5C_{35}$	167	89	55.0	222.0	171	0.06
$M_{60}O_0C_{40}$	168	92	78.0	442.6	180	0.10
MNPs–$M_{60}O_{35}C_5$	174	75			174	0.11
MNPs–$M_{60}O_{20}C_{20}$	166	82			166	0.11
MNPs–$M_{60}O_5C_{35}$	170	85			172	0.08
MNPs–$M_{60}O_0C_{40}$	185	84			189	0.12

[a)]MNPs, magnetic nanoparticles; M, methyl methacrylate; O, oleic acid; C, Crodamol; at different weight percent indicated by the number subscribed.

3. Results and Discussions

In order to study the effect of costabilizers in the polymerization kinetics, some experiments without MNPs were carried out with analogous composition of the organic phase than the experiments with MNPs. **Table 1** summarizes the global results for all the experiments. The selected codes for the different runs include the abbreviations "M," "O," and "C", representing to MMA, OA, and Crodamol, respectively; with a subscript that indicates each wt% in the organic phase. Thus, $M_{60}O_{35}C_5$ represents the experiment with an organic phase composed of 60 wt% of MMA, 35 wt% of OA, and 5 wt% of Crodamol. When MNPs were incorporated, the abbreviation MNPs was also included at the beginning of the code.

The initial d_d ranged between 166 and 185 nm for all the experiments, obtaining final d_p in a similar range (Table 1), suggesting that droplets nucleation was the main site of nucleation. In addition, the incorporation of MNPs in PMMA nanocapsules did not produce significant differences on d_d and d_p (Table 1), which indicates that the fusion/fission events occurring during miniemulsification did not change in the presence of MNPs. Also, the low PDI values, around 0.1, obtained by DLS, indicate that all latexes have narrow size distributions.

Figure 1 shows the monomer conversion (x) for the experiments without (Figure 1a) and with MNPs–OA (15% wbm) incorporated in PMMA nanocapsules (Figure 1b). In both cases, the increase of OA content in the organic phase composition reduced the polymerization rate and the final conversion obtained after 6 h of reaction (Table 1). This behavior is rather expected because the radical attack on the double bond of OA (OA is a monounsaturated fatty acid) generates more stable radicals, with lower propagation constant. Thus, increasing OA content leads to slower kinetics and to lower molecular weights (M_n and M_w in Table 1). It has to be mentioned that Crodamol and OA did not appear in the molecular weight distribution since their molar mass are below those of the standards used in the calibration curve. A similar behavior has been observed for the miniemulsion polymerization of MMA with castor oil[16,17] or andiroba oils[18] used as costabilizers.

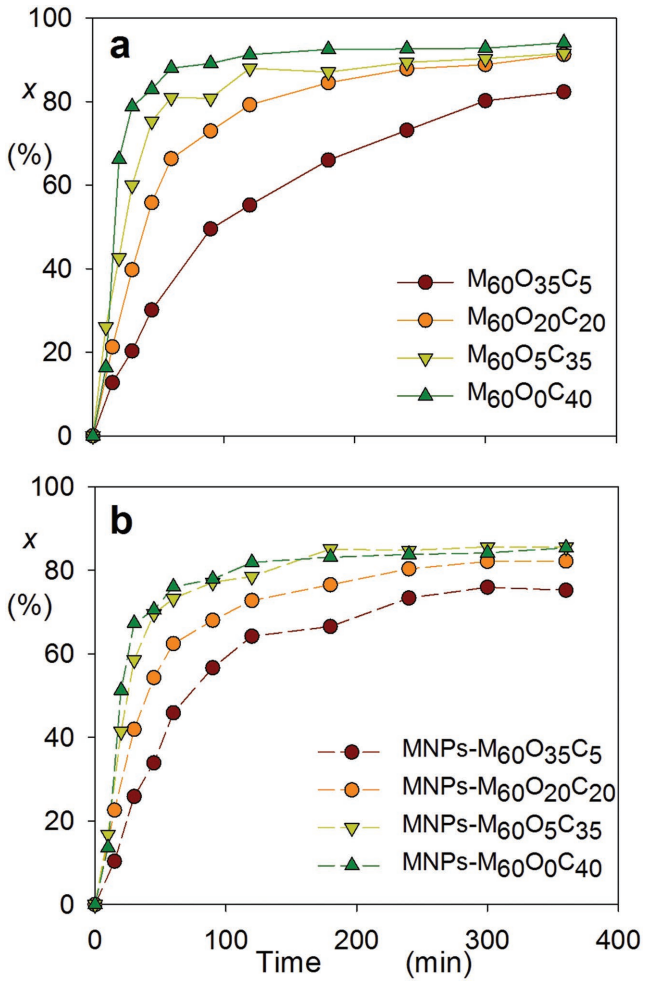

Figure 1. Evolution of conversion in the miniemulsion polymerization of MMA using varied contents of OA and Crodamol as costabilizers in absence MNPs–OA (a), and in the presence of 15% wbm of MNPs–OA (b).

In addition, lower polymerization rates and final conversions were observed in experiments carried out in the presence of MNPs, respect to the analogous ones with the same organic phase composition. This could be due to either the presence of additional OA on MNPs, or the reduction in the concentration of free radicals in the polymerization medium due to their reaction with part of the magnetite (Fe_3O_4), converting it to Fe_2O_3.[21] The residual monomer might have a deleterious effect on the final biomedical application.[27] Therefore, the nanocapsules should be lyophilized previously to its application in order to remove the residual monomer.

The incorporation of MNPs in PMMA nanocapsules was first confirmed with FT-IR analyses (**Figure 2**). The characteristic band at 590 cm^{-1}, corresponding to stretching vibration of Fe—O bond of Fe_3O_4,[10,26] can be observed in the spectra of MNPs–$M_{60}O_0C_{40}$ sample. In addition, the adsorption at 1736 cm^{-1} corresponds to the stretching of C=O groups present in PMMA and Crodamol, and the bands in the 3000–2800 cm^{-1} region are attributed to the stretching of C—H bonds of the saturated alkane.

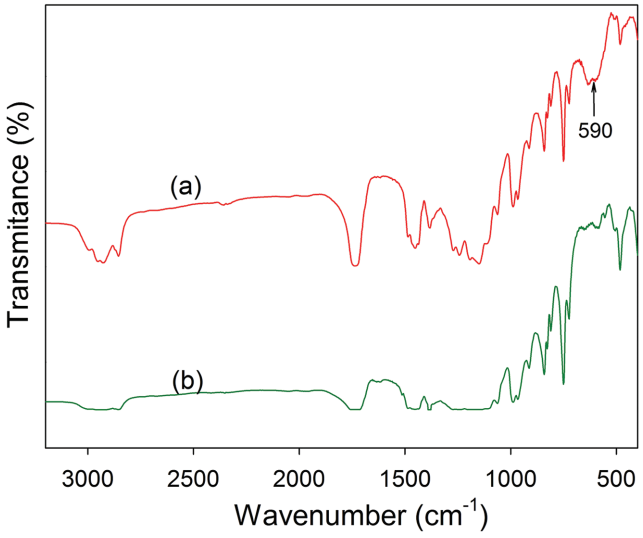

Figure 2. FT-IR spectra of experiments MNPs–$M_{60}O_0C_{40}$ a) and $M_{60}O_0C_{40}$ b).

The nanocapsules morphology was observed by TEM (**Figure 3**) for the experiments without OA and with 5% and 20% of OA. The experiments with 35% of OA were not characterized as they presented much lower conversion when compared to the others. When higher OA content (20%) was employed only a reduced number of particles presented the nanocapsules morphology and most of them were nanospheres. The same behavior was observed for nanocapsules containing MNPs or not as it is shown in more detail in Figure 3a–c. Besides, much lower phase segregation would be expected in this sample synthesized with higher OA content, as the reaction of PMMA-radical with the OA creates covalent bonds between PMMA and OA, increasing the compatibility between the polymer and the costabilizer and reducing phase separation inside the particles during polymerization. On the other hand, when Crodamol was the main costabilizer, most of the nanoparticles presented very clear nanocapsules morphology (Figure 3d–h). In the TEM images, the presence of MNPs into the nanocapsules are shown as black points. Notice that MNPs–OA synthesized with the method previously described exhibited a small size, of around 5–13 nm in diameter, with narrow size distribution.[10] It

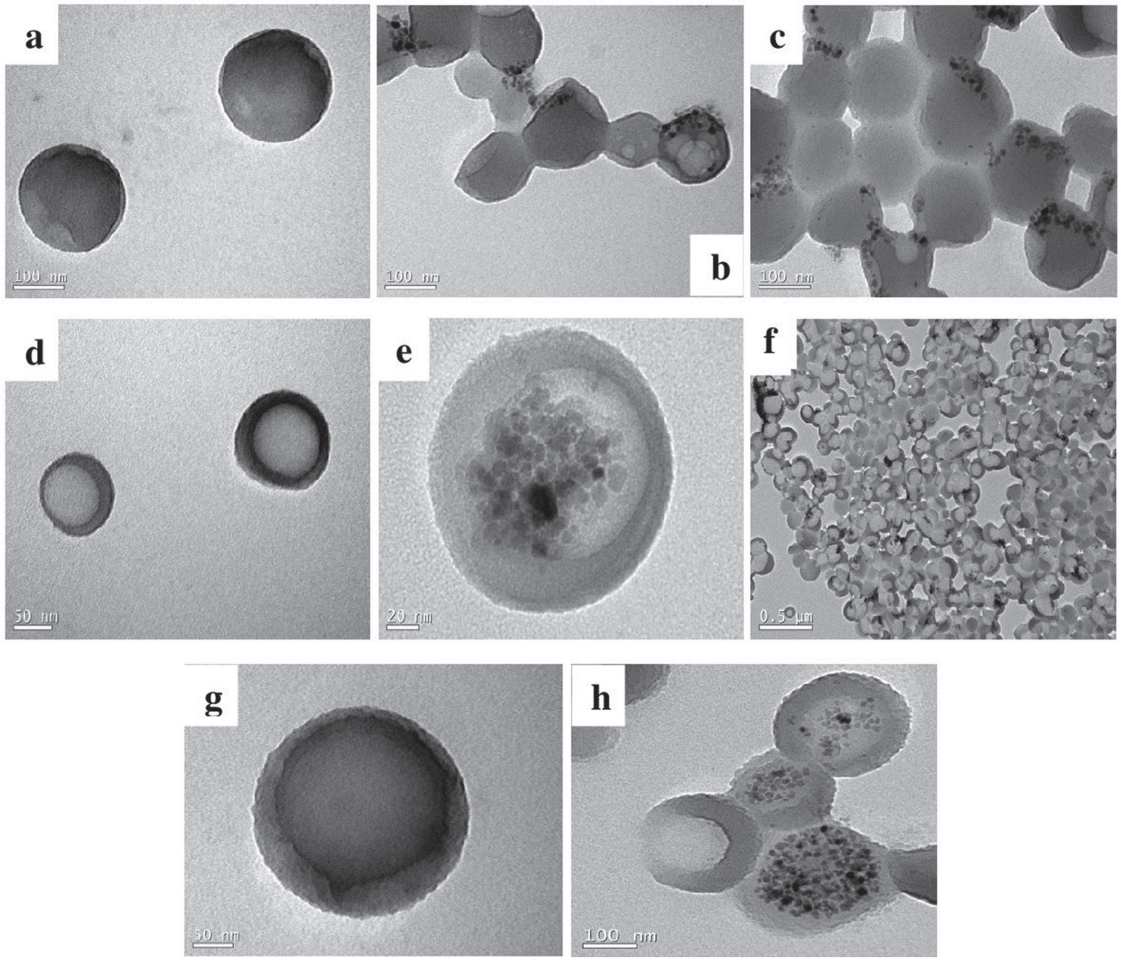

Figure 3. TEM images of PMMA nanoparticles for the experiments $M_{60}O_{20}C_{20}$ (a), MNPs–$M_{60}O_{20}C_{20}$ (b,c), $M_{60}O_5C_{35}$ (d), MNPs-$M_{60}O_5C_{35}$ (e,f), $M_{60}O_0C_{40}$ (g), and MNOs–$M_{60}O_0C_{40}$ (h).

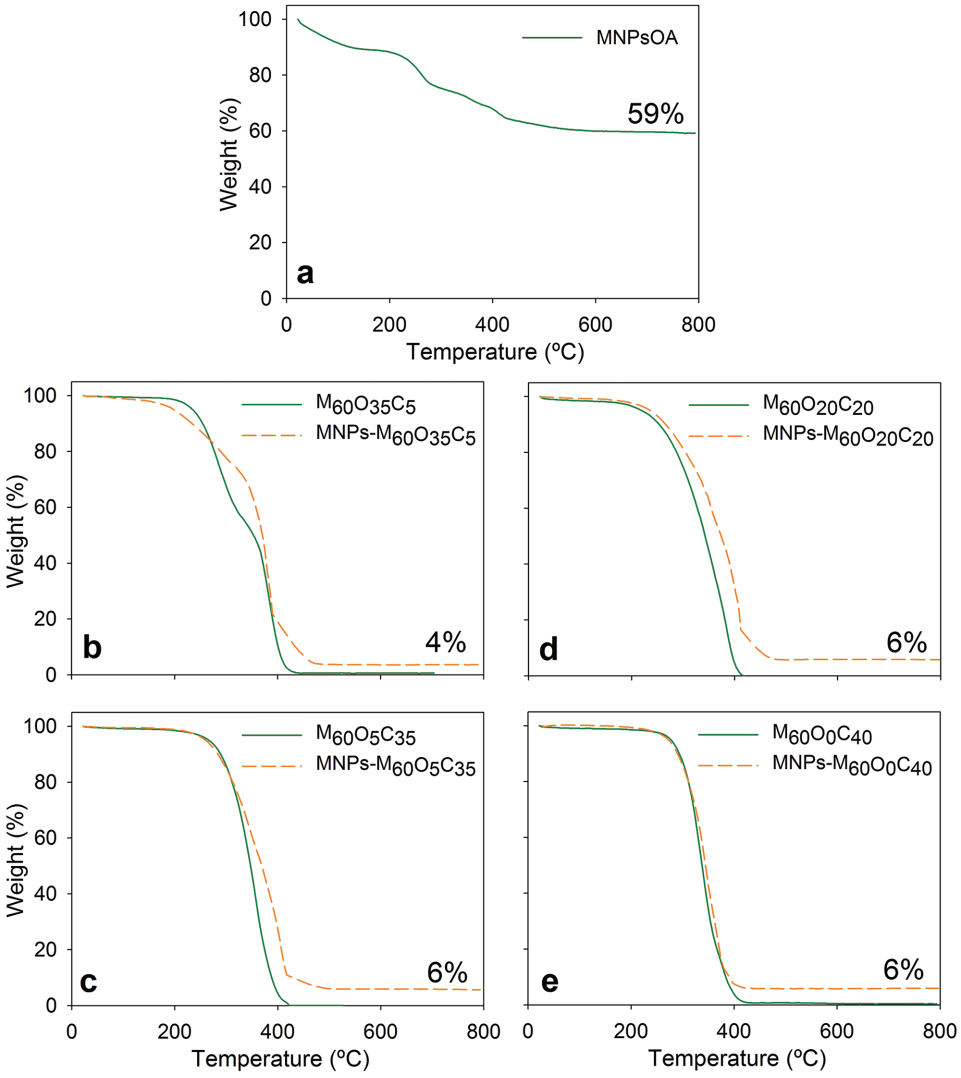

Figure 4. TGA thermograms obtained for pure MNPs–OA (a), and PMMA nanocapsules with and without MNPs (b–e).

is also possible to observe in Figure 3 that MNPs stayed in the liquid core in nanocapsules with up to 5% of OA content and were displaced for the polymer shell at higher OA content.

The thermal decomposition of pure MNPs–OA and PMMA nanocapsules were studied by TGA. For pure MNPs–OA, **Figure 4**a shows a mass loss of 10% in the temperature range 0–100 °C that is attributed to the presence of impurities and/or water. Other two mass losses occurred in the MNPs–OA sample between temperatures of 200 and 530 °C, with a total mass loss of 30%. The first one is related to free OA, and the second one is associated to the OA adsorbed onto the MNPs.[21] The residual concentration of 59% corresponds to the MNPs. In the case of PMMA nanocapsules without MNPs, all the sample was completely degraded when reaching about 480 °C, such as can be observed in Figure 4b–e. On the other hand, TGA analysis of experiments with MNPs showed a residual concentration between 4% and 6% (values indicated over the dashed TGA thermograms in Figure 4b–e), corresponding to MNPs incorporated in PMMA nanocapsules. These values are indicative of an efficient encapsulation of MNPs in all experiments, considering the 15% wbm of MNPs–OA employed in the recipe with an iron oxide content of 59%, determined by TGA, and the measured gravimetric monomer conversion (73–92%, Table 1).

The magnetic properties of MNPs–PMMA nanocapsules were characterized by VSM. **Figure 5** shows the hysteresis loops as a function of the magnetic field at room temperature. Saturation magnetization (Ms), Ms = M(H = 20 kOe), and remnant magnetization (Mr) values in emu g^{-1} of iron oxide were obtained considering the iron oxide mass obtained from TGA analysis. As can be observed in **Table 2** and Figure 5, all nanocapsules with MNPs presented super-paramagnetic behavior at room temperature, and absence of hysteresis loop, with small Mr/Ms ratio and coercive field (Hc).[28–30] As observed in Table 2, the Ms values of the MNPs-PMMA nanocapsules were significantly smaller than that of MNPs–OA (Ms = 66 emu g^{-1}).[10] The decrease in Ms may be due to oxidation processes during sonication or during the polymerization because of the presence of

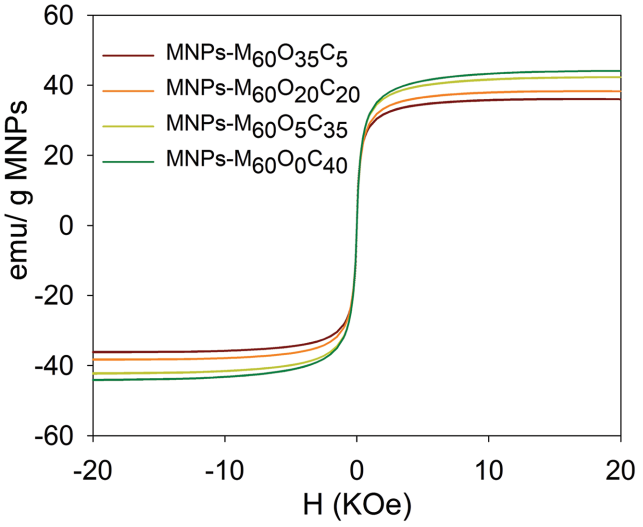

Figure 5. Magnetization curves of different MNPs–PMMA nanocapsules.

oxidizing initiator fragments, which leads to the formation of some iron oxides without magnetization or with low Ms, such as maghemite (Fe_2O_3), which has a lower Ms of 60–80 emu g^{-1} compared to 92–100 emu g^{-1} for Fe_3O_4.[21,25,31] Similar behavior was observed by Feuser et al.[10] when encapsulating MNPs in PMMA nanospheres via miniemulsion polymerization. Other works, also related a decreased of Ms value when MNPs were encapsulated in polymeric microparticles and nanoparticles.[25,32] However, the observed Ms values are enough to allow the separation from the aqueous phase of encapsulated MNPs when an external magnetic field is applied, as can be seen in **Figure 6**.

4. Conclusions

The effect of costabilizers composition (OA and Crodamol) in the incorporation of MNPs in PMMA nanocapsules by miniemulsion polymerization was investigated. Results showed that high OA content reduced the polymerization rate, the PMMA molecular weights and affected the nanocapsules morphology due to the reaction of PMMA-radical with the unsaturation of the oleic acid. Reducing the amount of OA and using Crodamol as the main costabilizer increased the polymerization rate, conversion and favored the incorporation of the MNPs to the liquid core of the nanocapsules. Finally, super-paramagnetic properties were observed for MNPs–PMMA nanocapsules showing their ability to be attracted by an external magnetic field, making them attractive for drug delivery to specific cells or tissues without damaging healthy cells. Future studies of application of MNPs–PMMA nanocapsules, such as, encapsulation of drugs for cancer treatment and in vitro cytotoxicity assay, as well as, cancer treatment by hyperthermia will be underway.

Table 2. Magnetic properties of MNP–PMMA nanocapsules.

Experiment	Ms (emu g^{-1} MNPs)	Mr (emu g^{-1} MNPs)	Hc (Oe)	Mr/Ms
MNP–$M_{60}O_{35}C_5$	36	0.08	0,6	2.2×10^{-3}
MNP–$M_{60}O_{20}C_{20}$	38	0.05	0,5	1.3×10^{-3}
MNP–$M_{60}O_5C_{35}$	42	0.06	0,4	1.4×10^{-3}
MNP–$M_{60}O_0C_{40}$	44	0.04	0,4	0.9×10^{-3}

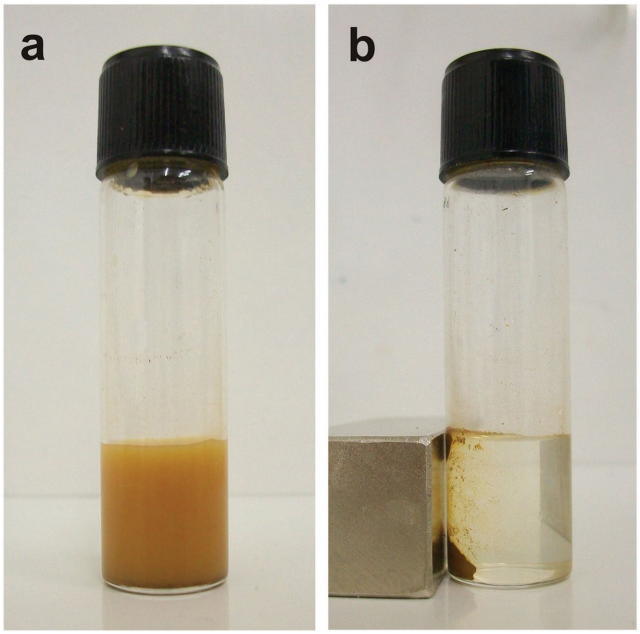

Figure 6. MNPs–PMMA nanocapsules in distilled water without application of an external magnetic field (a) and with application of an external magnetic field (b).

Acknowledgements

The authors would like to thank: Secretary of University Policies of the Ministry of Education of Argentina, Universidad Nacional del Litoral (UNL, Argentine), Consejo Nacional de Investigaciones Cientificas y Tecnicas (CONICET, Argentina), Conselho Nacional de Desenvolvimento Científico e Tecnológico (CNPq–Brazil) and Coordenação de Aperfeiçoamento de Pessoal de Nível Superior (CAPES–Brazil) for financial support; Laboratório Central de Microscopia Eletrônica at the Universidade Federal de Santa Catarina (LCME-UFSC) for TEM images and Laboratorio Multiusuário de Caracterização Magnética de Materiais at Universidade Federal de Santa Catarina. (LMCMM-UFSC) for the magnetic characterization.

Conflict of Interest

The authors declare no conflict of interest.

Keywords

fatty acids, miniemulsion polymerization, polymeric nanocapsules, super-paramagnetic nanoparticles

Received: August 25, 2017
Revised: November 3, 2017
Published online:

[1] A. K. Gupta, M. Gupta, *Biomaterials* **2005**, *25*, 3995.
[2] A. S. Teja, P. Y. Koh, *Prog. Cryst. Growth Charact. Mater.* **2009**, *55*, 45.
[3] S. Laurent, D. Forge, M. Port, A. Roch, C. Robic, V. L. Elst, R. N. Muller, *Chem. Rev.* **2010**, *108*, 2010.
[4] C. S. S. R. Kumar, F. Mohamad, *Adv. Drug Delivery Rev.* **2011**, *63*, 789.
[5] J. Shi, X. Yu, L. Wang, Y. Liu, J. Gao, J. Zhang, R. Ma, R. Liu, Z. Zhang, *Biomaterials* **2013**, *34*, 9666.
[6] K. S. Tang, S. M. Hashmi, E. M. Shapiro, *Nanotechnology* **2013**, *24*, 125101.
[7] M. Koneracka, M. Muckova, V. Zavisova, V. Tomasovicova, P. Kopcanski, M. Timko, A. Jurikova, K. Csak, V. Kavecansky, G. Lanes, *J. Phys.* **2008**, *20*, 240.
[8] A. Shakeri-Zadeh, M.-B. Shiran, S. Khoee, A. M. Sharifi, H. Ghaznavi, S. Khoei, *J. Biomater. App.* **2014**, *29*, 548.
[9] A. P. Romio, H. H. Rodrigues, A. Peres, A. D. C. Viegas, E. Kobitskaya, U. Ziener, K. Landfester, C. Sayer, P. H. H. Araújo, *J. Appl. Polym. Sci.* **2013**, *129*, 1426.
[10] P. E. Feuser, L. Santos Bubniak, M. C. Santos Silva, A. Cas Viegas, A. Castilho Fernandes, E. Ricci-Junior, M. Nele, A. C. Tedesco, C. Sayer, P. H. H. Araújo, *Eur. Polym. J.* **2015**, *68*, 355.
[11] P. E. Feuser, A. C. Fernandes, M. Nele, A. Cas Viegas, E. Ricci-Junior, M. Nele, A. C. Tedesco, C. Sayer, P. H. H. Araújo, *Colloids Surf., B.* **2015**, *135*, 357.
[12] M. R. Ruggiero, S. G. Crich, E. Sieni, P. Sgarbossa, M. Forzan, E. Cavallari, R. Stefania, F. Dughiero, S. Aime. *Nanotechnology* **2016**, *27*, 285104.
[13] J. Liu, Y. Kitamoto, *Jpn. J. Appl. Phys.* **2016**, *55*, 02BE02.
[14] K. Landfester, A. Musyanovych, V. Mailander, *J. Polym. Sci.: Part A: Polym. Chem.* **2010**, *48*, 493.
[15] M. Bathfield, C. Graillat, T. Hamaide, *Macromol. Chem. Phys.* **2005**, *206*, 2284.
[16] A. P. Romio, N. Bernardy, E. L. Senna, P. H. H. Araújo, C. Sayer, *Mater. Sci. Eng., C* **2009**, *29*, 514.
[17] F. R. Steinmacher, N. Bernardy, J. B. Moretto, E. I. Barcelos, P. H. H. Araújo, C. Sayer, *Chem. Eng. Technol.* **2010**, *33*, 1877.
[18] P. B. Cardoso, P. H. H. Araújo, C. Sayer, *Macromol. Symp.* **2013**, *324*, 114.
[19] M. F. Cury-Boaventura, C. Pompéia, R. Curi, *Clin. Nutr.* **2004**, *23*, 721.
[20] M. F. Cury-Boaventura, C. Pompéia, R. Curi, *J. Nutr.* **2005**, *21*, 395.
[21] K. Landfester, L. P. Ramires, *J. Phys.* **2003**, *15*, 1345.
[22] A. R. Mahdavian, M. Ashjari, H. S. Mobarakeh, *J. Appl. Polym. Sci.* **2008**, *110*, 1242.
[23] V. Chiaradia, A. Valério, P. E. Feuser, D. Oliveira, P. H. H. Araújo, C. Sayer, *Colloids Surf., A* **2015**, *482*, 596.
[24] S. Gyergyek, D. Makovec, A. Mertelj, M. Huskic, M. Drofenik, *Colloids. Surf., A* **2010**, *366*, 113.
[25] R. Y. Hong, B. Feng, X. Cai, G. Liu, H. Z. Li, J. Ding, Y. Zheng, D. G. Wei, *J. Appl. Polym. Sci.* **2009**. *112*, 89.
[26] P. E. Feuser, J. M. C. E. L. Arévalo Junior, G. R. Rossi, E. da Silva Trindade, M. E. M. Rocha, A. V. Jacques, E. Ricci-Júnior, M. C. Santos-Silva, C. Sayer, P. H. H. Araújo, *J. Mater. Sci.: Mater. Med.* **2016**, *27*, 185.
[27] M. A. Pembertom, B. S. Lohmann, *Regul. Toxicol. Pharmacol.* **2014**, *69*, 467.
[28] C. K. Weiss, K. Landfester, *Adv. Polym. Sci.* **2010**, *233*, 185.
[29] V. V. Mody, A. Cox, S. Shah, A. Singh, W. Bevins, H. Parihar, *Appl. Nanosci.* **2014**, *4*, 385.
[30] P. Chandrasekharana, D. Maity, C. X. Yongc, K.-H. Chuang, J. Ding, S.-S. Feng, *Biomaterials* **2011**, *32*, 5663.
[31] P. Dallas, V. Georgakilas, D. Niarchos, P. Komninou, T. Kehagias, *Nanotechnology* **2006**, *17*, 2046.
[32] H. Zhao, K. Saatchi, U. O. Hafeli, *J. Magn. Magn. Mater.* **2009**, *321*, 1356.

